



Fluidized bed chemical looping for CO₂ capture and catalytic methanation using dual function materials

Fiorella Massa^a, Elisabetta Maria Cepollaro^a, Stefano Cimino^a, Antonio Coppola^a, Fabrizio Scala^{a,b,*}

^a STEMS, CNR, P.le Tecchio 80, 80125, Napoli, Italy

^b DICMaPI, Università di Napoli Federico II, P.le Tecchio 80, 80125, Napoli, Italy

ARTICLE INFO

Keywords:

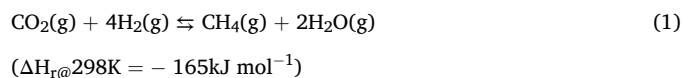
CO₂ Capture
Methanation
Dual function materials
Fluidized beds
Chemical looping

ABSTRACT

CO₂ capture from combustion flue gas combined to its catalytic hydrogenation to synthetic methane is considered as a promising technology in the field of Carbon Capture and Utilization (CCU). In this work, the integrated CO₂ capture and methanation process was investigated in an innovative chemical looping configuration using dual function materials (DFMs) recirculated alternately between two interconnected bubbling fluidized bed reactors. By physically separating the CO₂ capture step and the catalytic hydrogenation reaction in two coupled fluidized bed reactors it is possible to effectively control and independently optimize the operating temperature of each half cycle while running the process continuously. A high-performing Lithium-Ruthenium/Al₂O₃ was selected to investigate the effect of the specific temperature level for the CO₂ capture and the methanation phases in the range 200 - 400 °C, checking the stability and repeatability of the CO₂ sorption and catalytic performance over 5 repeated cycles for each operating condition. Subsequently, under the best conditions in terms of methanation performance, a similar Na-promoted dual function material was also tested. The DFMs performance appeared to be quite reproducible over the cycles, but it was subject to kinetic limitations, especially in the case of Na-Ru/Al₂O₃. Interestingly, the methane yield approached 100 % under the highest tested temperatures for the Li-based DFM. Despite some limitations due to the experimental purge phases of the lab-scale system, the study provides the proof-of-concept of the process which enables the possibility of decoupling the two steps with the aim of a large potential intensification.

1. Introduction

In the framework of the efforts made to address the climate change, the reduction of CO₂ emissions is one of the key goals. Among the different technological options, Carbon Capture and Utilization (CCU) is regarded as one of the most promising. This approach, if considering CO₂ methanation, may be combined to a power-to-gas technology, which is interesting in the context of energy transition. It entails the possibility of realizing a chemical energy storage using renewable hydrogen, and exploiting the surplus of renewable electric energy [1], through the production of synthetic methane via the reaction:



This promising solution has been applied on an industrial scale in the

Audi motor company's "e-gas" facility in Werlte (Germany), where 1000 t/year of synthetic natural gas (SNG) are produced using concentrated CO₂ from a nearby biogas plant [2]. Synthetic methane production is gaining increasing interest since this fundamental energy carrier benefits from an already existing distribution grid, through which it can be easily handled and transported, and good social acceptance. One of the main drawbacks of current carbon capture technologies lies in energy-intensive regeneration processes. Typical carbon capture processes rely on the CO₂ absorption by corrosive amine solutions such as monoethanolamine (MEA) ones, or on the adsorption by solids, generally alkaline metal oxides, which require high temperature thermal swing for the regeneration step [2]. A CO₂ capture process would imply an increase by 40 to 80 % of the total capital cost for conventional post-combustion carbon capture and storage (CCS), with only the capture step estimated to increase the energy requirements of a power plant by 25–40 % [3]. Additionally, logistics and energy penalties due to the

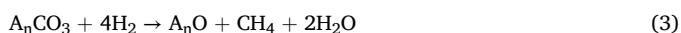
* Corresponding author.

E-mail address: fabrizio.scala@unina.it (F. Scala).

handling and transport of concentrated CO₂ to underground injection facilities or processing plants must be considered [2].

Integrated CO₂ capture and reduction (ICCR) solutions have been recently proposed to reduce the cost and make the whole process more efficient [4–6]. These techniques are based on the use of dual function materials (DFM), which combine both sorbent and catalyst to capture and convert CO₂ from a point source (e.g. combustion flue gases, anaerobic digestion, etc.) into CH₄ exploiting the reduction with green (renewable) H₂, and resulting in a chemical looping process. DFMs include alkaline or alkaline earth components as a supported adsorbent for CO₂ capture (e.g., Na or Ca), and Ni or Ru as the catalytically active phase for CO₂ hydrogenation. The selective CO₂ capture on DFMs and the hydrogenation of the captured CO₂ are performed alternately.

The two reaction steps involved can be schematized as [7]:



where, A = Li, Na, K, Ca, or Mg; and n = 1 or 2.

The DFM characteristics and performance are the keys to the success for such emerging chemical looping processes: high catalytic activity and selectivity and easy reducibility, mechanical stability and durability under cyclic operation, large CO₂ capture capacity and easy desorption are required [8]. Ni-based catalysts, the most used in industrial applications due to their high activity combined to a low price, are characterized by easy oxidation during the adsorption phase, being, on the contrary, difficult to reduce at low temperature. Therefore, the optimal catalyst for these applications has been found to be Ru supported on alumina showing easy reducibility at low temperature, coupled with favorable interaction with alkali-based sorption phases in DFMs [8]. High loadings of active metals in the DFM should be avoided to reduce the cost as well as to limit the parasite H₂ consumption for the reduction of their oxides during each methanation cycle [7]. Several alkali/alkaline-earth oxides/carbonates (mostly those of Li, Na, K, Ca, Mg, Ba, La, Ce) have been investigated as CO₂ sorbent phases at intermediate temperatures (200–450 °C). As for the Ru-based catalysts, Na₂O/Na₂CO₃ has been suggested as the best sorbent material [9,10]. However, another study, considering a 5 % Ru/Al₂O₃ catalyst, reported the following order of activity for alkali metals: Cs ≥ Li > Rb > Na ≥ K [11]. Based on this finding, Cimino et al. [12] developed a Li-promoted Ru/Al₂O₃ DFM, outperforming the Na- and K- promoted counterparts, considering both CO₂ capture and methanation steps. They pointed out the formation of superficial Li-aluminates, which likely prevent the formation of stable carbonate species, reported for the other metals investigated, which are difficult to hydrogenate and negatively affect the methanation performance.

In this work, we prepared two Ru-based DFMs containing a low loading of noble metal (1 %) dispersed together with 5 % Li or Na on commercial γ-Al₂O₃ spheres characterized by high mechanical resistance. To date, the ICCR concept has been only investigated in fixed-bed reactors involving periodic switching of the inlet feed (CO₂ rich stream/H₂). On the contrary, herein we propose an innovative chemical looping

process based on the use of two interconnected fluidized beds (Fig. 1). Such configuration would allow a steady operation of the process, where the DFM particles can be continuously transported between a CO₂ capture reactor and a methanation reactor, thus overcoming one of the main drawbacks of fixed beds, due to their inherent discontinuous operation. Furthermore, taking advantage of their outstanding heat transfer characteristics and low pressure drops, the two interconnected fluidized bed reactors could be run at different temperature levels independently optimized to maximize both the CO₂ capture and the methanation.

2. Experimental

2.1. Materials

The two DFMs were prepared following the procedure reported by Cimino et al. [8,12], since the addition of the sorbent material on the catalyst phase was shown to produce more effective DFMs. The materials were prepared by dispersing 1 %_{wt} of Ruthenium by incipient wetness impregnation of a Ru(III) nitrosyl nitrate solution on commercial attrition-resistant 0.6 mm γ-Al₂O₃ spheres (190 m²/g, provided by Sasol). The impregnated material was dried at 120 °C and then calcined in air at 350 °C for 1 h. Then, the alkali sorbents, Li or Na (5% wt), were uniformly dispersed inside γ-Al₂O₃ particles by two repeated incipient wetness impregnations with appropriate alkali nitrate solutions followed by a final reduction under 20 %H₂ at 450 °C for 2 h.

2.2 Characterization of DFMs

Temperature-Programmed Surface Reaction tests (H₂-TPSRx) of CO₂ pre-adsorbed on the DFMs were performed in a Setaram Labsys Evo TGA-DTA-DSC 1600 flow microbalance. DFM samples (70–80 mg) were reduced at 400 °C for 1 h under a 4.5 %H₂/Ar flow and cooled under Ar to room temperature, where CO₂ (19% vol. in N₂ at 50 cm³ min⁻¹) was adsorbed for 1 h. Thereafter, the sample was purged and eventually heated up to 650 °C at a rate of 10 °C min⁻¹ under a flow of 4.5 % H₂/Ar (at 50 cm³ min⁻¹). The evolved gases were continuously analyzed by a Mass Spectrometer (Pfeiffer Thermostar G) equipped with a Secondary Electron Detector (MS-SEM), recording the temporal profiles at m/z = 2 (H₂), 15 (CH₄), 18 (H₂O), 28 (CO), 44 (CO₂).

In-situ DRIFTS was performed to study CO₂ adsorption on both DFMs using a Perkin Elmer Spectrum 3 equipped with a MCT detector at 4 cm⁻¹ resolution. Powdered samples were loaded in a heated chamber (PiKe DRIFT) and pre-treated in-situ under 25 %H₂/Ar flow at 360 °C for 1 h. After cooling down to the desired temperature under Ar flow, a background spectrum was collected. Thereafter, adsorption was performed by flowing a 15 %CO₂/N₂ mix for 10 min, followed by Ar purging for 15 min.

Additional characterization of the two DFMs can be found in our recently published works [8,12].

2.3 Apparatus for ICCR

The experimental campaign was carried out in a batch lab-scale apparatus, the Twin Beds system, consisting of two identical stainless steel bubbling fluidized beds, shown in Fig. 2, connected to each other by a duct enabling the fast pneumatic transfer of solid materials [13].

Each reactor is composed of 3 sections: the wind-box, 0.66 m high, filled with metal elements and acting as a pre-heater/pre-mixer, the 1 m high fluidization column and, in the upper part, a system of a three-way valve that can be connected to the gas analyzers. This apparatus was conceived with the aim of studying looping processes: it enables the pneumatic transport of granular material in about 5 s between the two reactive environments by means of a connecting tube (ID 10 mm) immersed in both reactors. The fluidization column and the wind-box are made of a tubular steel element (AISI 316) with an internal

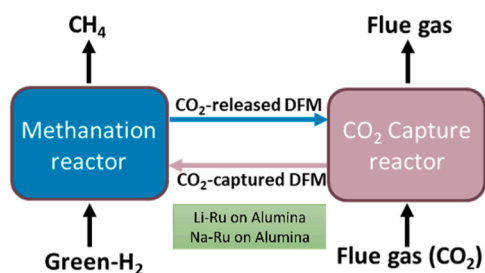


Fig. 1. Reactor configuration for ICCR using dual function materials with fluidized bed chemical looping.

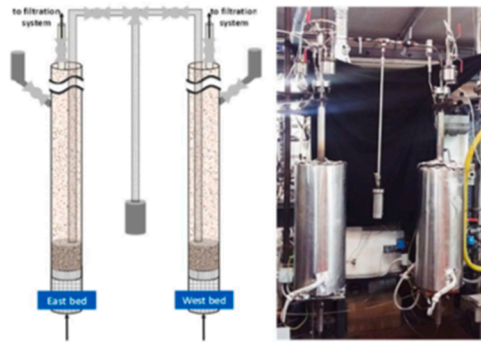


Fig. 2. Twin Beds Apparatus.

diameter of 40 mm. In between the two sections, connected by a flange, a perforated plate is located to uniformly distribute the gas inside each reactor. A hopper is placed on the top of each reactor to carry out the bed loading. The electrical heating system consists of two semi-cylindrical furnaces on each reactor (Watlow, Ceramic Fiber Heaters) with a heating length of 457 mm and a power per semi-cylinder of 2100 Watts. A PID controller (Watlow, EZ-Zone ST) is connected to each bed via a K-type thermocouple (Cr-Al) inserted 40 mm above the distribution plate. During the tests, the output concentration of the species was measured by a continuous gas analyzer (MRU VARIO LUXX) able to detect CH₄, CO, CO₂ by means of NDIR detectors and H₂ via a TCD. The pneumatic transport of the solids between the two reactors was carried out generating an overpressure by means of a system of valves that enables and modulates the flow of the material. Specifically, as for the transport duct, three valves are present on it: two ball valves close to each reactor, which modulate the flow through the duct and a centrally located three-way valve connected to a discharge duct, which allows to direct the material either between the two reactors or towards the discharge vessel. Above each reactor, another valve allows the outlet gas to be sent to the analyzer system and the vent.

2.4. Procedure

CO₂ capture and the subsequent methanation were investigated in batch experiments at the temperatures of 200, 300 and 400 °C and 230, 265 and 300 °C, respectively. The DFM carbonation cycles were all performed in one reactor, while the hydrogenation/regeneration ones in the other reactor. Once the set temperature was reached, the material was loaded into the carbonation reactor, where a bed of inert silica in the size 800–900 μm was already fluidized at a fluidization velocity of 0.5 m/s. The presence of silica sand was necessary to keep temperature variations to a minimum and to assure the segregation of DFM particles to the top of the bed [14]. After the loading of DFM (about 20 g), 5 % CO₂ in N₂ stream was fed to the reactor for 8 min (carbonation) followed by purging 2 min in pure N₂ before the DFM was transferred to the other reactor. The hydrogenation in the second reactor, which was already fluidized by N₂, started once the transfer of the material was completed: a flow of 4 % H₂ in N₂ was fed for a total duration of 8 min, followed by 2 min of N₂ purging. Then the DFM was transferred back to the carbonation reactor. Five complete cycles of carbonation and hydrogenation were carried out for each test condition.

The progress of the methanation steps was monitored by measuring the concentration of the main species in the outlet gases. The molar flows of the species of interest were calculated as follows:

$$F_i^{OUT}(t) = c_i^{OUT}(t) \cdot F_{tot}^{OUT}(t) \quad (4)$$

$$F_{tot}^{OUT}(t) = \frac{F_{N_2}}{c_{N_2}(t)} \cdot 100 \quad (5)$$

where F_i^{OUT} indicates the molar flow of the outlet species ($i = \text{H}_2, \text{CO}_2,$

CH₄, CO), c_i^{OUT} their concentration in the stream and F_{tot}^{OUT} the total molar flow exiting the reactor. The latter, from (5), was calculated through the nitrogen balance, being F_{N_2} and c_{N_2} its molar flow and outgoing concentration, respectively. The total outlet molar amounts of the species could be calculated along a certain time interval ($0-t_f$) discretizing the following integral and replacing it by the summation:

$$n_i^{OUT} = \int_0^{t_f} F_i^{OUT}(t) dt \approx \sum_{j=0}^{t_f} F_i^{OUT}(j) \cdot \Delta j \quad (6)$$

with Δj the sampling time interval of the signal (1 s).

CH₄ yield and selectivity and CO₂ conversion in the methanation reactor were calculated based on the total carbon-species released according to the following definitions, having excluded the formation of traces of C₂₊ hydrocarbons [8,10]:

$$Y_{CH_4} = n_{CH_4}^{OUT} / (n_{CH_4}^{OUT} + n_{CO_2}^{OUT} + n_{CO}^{OUT}) \quad (7)$$

$$S_{CH_4} = n_{CH_4}^{OUT} / (n_{CH_4}^{OUT} + n_{CO}^{OUT}) \quad (8)$$

$$X_{CO_2} = 1 - n_{CO_2}^{OUT} / (n_{CH_4}^{OUT} + n_{CO_2}^{OUT} + n_{CO}^{OUT}) \quad (9)$$

where, obviously, $Y_{CH_4} = S_{CH_4} \cdot X_{CO_2}$.

3. Results

3.1 Characterization of DFMs

The addition of the Li or Na sorbent to a Ru/Al₂O₃ methanation catalyst is responsible for the CO₂ adsorption capacity of the DFMs. As shown in Fig. 3, both the pre-reduced DFMs can capture CO₂ already at room temperature with initially fast kinetics [8] (controlled by the external mass transfer in the thermobalance), giving almost overlapped

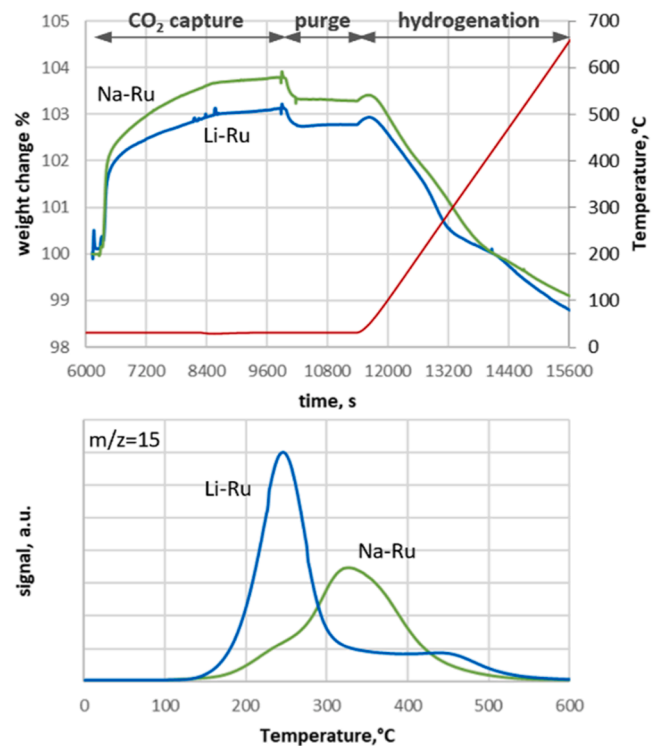


Fig. 3. TG-MS results during CO₂ adsorption at room temperature on reduced Li-Ru and Na-Ru DFMs and subsequent temperature programmed hydrogenation: a) temporal weight change of DFMs; b) Methane evolution as a function of temperature during the hydrogenation step.

temporal profiles. Thereafter, CO₂ adsorption continues at a much slower rate, with Na-Ru DFM showing a larger final weight gain (ca 3.8 %) w.r.t. its Li-Ru counterpart (ca 3.1 %). It is worth noticing that the true CO₂ capture capacity of the DFM cannot be directly calculated from thermo-gravimetric (TG) tests since the adsorption of CO₂ is generally associated to the simultaneous release of some water [8,10]. Part of the CO₂ captured was weakly bonded to the DFMs so that it was slowly removed during the subsequent isothermal purging step, as already reported for other alkali promoted Al₂O₃ sorbents [8]. Further amounts of weakly bonded CO₂ were thermally desorbed during the initial heating under H₂ flow, giving a characteristic peak centered at ca 100 °C (not shown). Fig. 3b shows that methane started to be formed by the reaction between H₂ and chemisorbed CO₂ from ca 130 °C. It clearly appears that the Li-Ru DFM was characterized by a much higher methanation activity than its counterpart, giving maximum CH₄ production at as low as 250 °C vs 335 °C required on the Na-Ru DFM. It can be argued that the peak of methane release resulted from the balance between the accelerating catalytic reaction and the corresponding consumption of the residual CO₂ stored on the DFM.

Moreover, the Li-Ru DFM gave 100 % selectivity to CH₄ up to 450 °C, whereas the Na-Ru sample also released some limited amounts of CO. This reflects the formation of more stable carbonate species on the surface of Na-Al₂O₃, which are more refractory to activate over the nearby Ru active sites. However, both DFMs were capable to recover their initial weight at $T \leq 400$ °C (Fig. 3a), suggesting a complete regeneration of their initial CO₂ capture capacity, which can be achieved due to the proximity between sorption and active sites at the nano-scale promoting fast spill-over effects. The further weight loss at higher temperatures was associated to the release of some CH₄ + CO and reflected the existence of residual, highly stable carbonate species on the DFMs which were far away from catalytic sites and could not effectively participate in the cyclic operation of the integrated capture-methanation process.

Fig. 4 presents the results of in-situ DRIFTS during CO₂ adsorption and subsequent purging at 280 °C over both DFMs. The two main bands in the region of carbonates (peaking at 1622, 1332 cm⁻¹ and 1605, 1376 cm⁻¹, respectively, for Na-Ru and Li-Ru DFMs) can be assigned to chemisorbed bi-dentate carbonates [8,10,15] which were readily formed upon exposure of both the pre-reduced DFMs to CO₂, thus confirming the fast kinetics of the capture process. A shoulder at 1550 cm⁻¹, associated to monodentate carbonates [8], was detectable especially for Na-Ru, which also showed signals in the 2050–1840 cm⁻¹ region due to

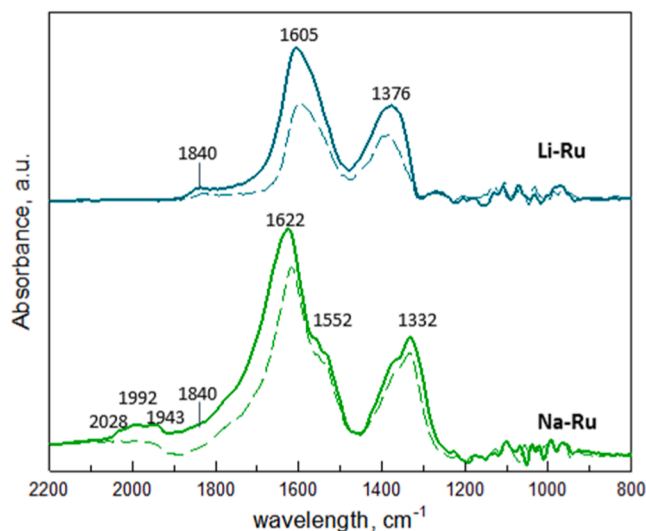


Fig. 4. In-situ DRIFT spectra for CO₂ adsorption over Li-Ru and Na-Ru DFMs at 280 °C (15 % CO₂/Ar flow for 10 min). Dashed lines represent the corresponding spectra following a 15 min purge under Ar flow.

the formation of various linear and bridged carbonyl species adsorbed on Ru [8,15]. In line with the results of TG experiments at lower temperatures, additional physisorbed bi-carbonate species (main signals at ca 1690, 1650 cm⁻¹) were formed more slowly over both DFMs during the capture stage under the CO₂ flow [8,10]. Those bicarbonates were weakly bonded to the surface and spontaneously desorbed during the 15 min purge under inert flow (dashed lines in Fig. 4). This desorption effect was proportionally more pronounced for the Li-Ru rather than for the Na-Ru DFM, which in turn retained a larger pool of more strongly adsorbed CO₂ species to be possibly hydrogenated in the subsequent step.

3.2 ICCR tests

Fig. 5 reports the normalized measured molar flows of outlet CH₄ as a function of time for a test using the Li-Ru/Al₂O₃ DFM. This figure refers to the test where both methanation and carbonation temperatures were set at 300 °C. Similar results were obtained at the other operating conditions. In Fig. 5 all the 5 hydrogenation half-cycles included in a complete ICCR test are depicted: in each case, CH₄ production shows a rapid increase reaching a maximum after 20–30 s followed by a slower decrease due to the progressive depletion of the captured CO₂ available on the DFM as reactant for methanation.

The DFM performance appeared quite stable and reproducible over the cycles, except for the first cycle where the residual presence of RuO_x on the DFM, which were promptly reduced to the catalytically active metal form, could slightly delay methane production.

The overall outlet amount of the gaseous species of interest was calculated by integration of the temporal concentration profiles, following the procedure described in the previous paragraph, and averaged over the last 4 cycles for all the tests performed. Fig. 6 summarizes the overall amount of outlet CH₄, in terms of mmol produced per gram of DFM, for all the test conditions.

As expected, for each carbonation temperature, methane production increased along with the increase of the methanation temperature from 230 to 300 °C due to the existence of kinetic limitations at low temperature. As for the effect of the CO₂-capture temperature, if considering the increase of carbonation temperature from 300 °C to 400 °C, it is evident that for all the methanation temperatures a decrease in the produced methane occurred. This is due to the exothermic nature of the CO₂ chemisorption, which is favored at lower temperatures where it can still proceed with fast kinetics. However, if considering the lowest carbonation temperature of 200 °C, a lower CH₄ production under all methanation conditions, compared to the case of the CO₂-capture at 300

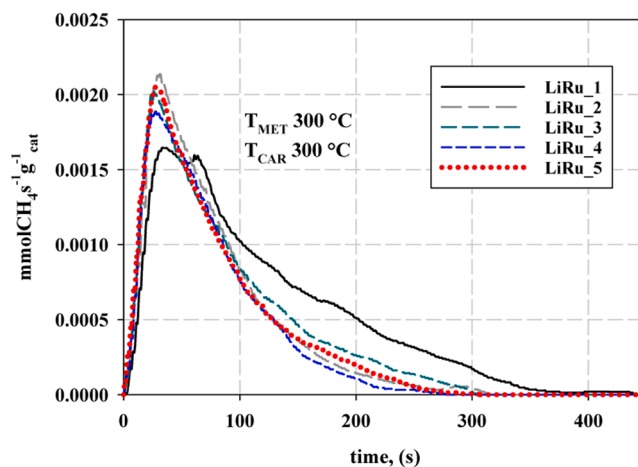


Fig. 5. Temporal normalized CH₄ outlet molar flow for the Li-Ru/Al₂O₃ test at methanation and carbonation temperatures of 300 °C. The curves refer to the 5 methanation cycles.

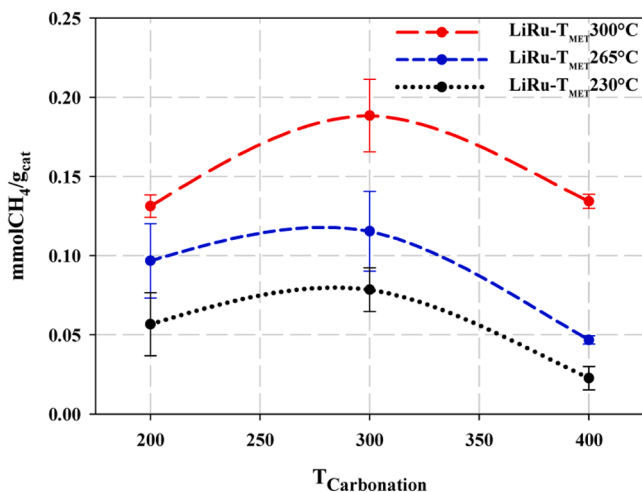


Fig. 6. Overall methane production under all the ICCR tests conditions with Li-Ru/Al₂O₃ DFM.

°C, occurred. This behavior is most likely attributable to the experimental procedure of the tests that determined a significant CO₂ stripping from the sorbent during the purge phase at the carbonation temperature of 200 °C. Under these conditions, the DFM material underwent a rapid temperature increase when transferred to the methanation reactor, which drove some thermal desorption of CO₂ during the purge before the reduction phase was started. This finding is supported by Fig. 7 where the overall amount of the measured carbon-containing species (CH₄+CO₂+CO) at the outlet is reported for the same tests shown in Fig. 6. When considering also the CO₂ detected at the outlet, the overall amount of carbon-containing species, in terms of mmol per gram of DFM material, decreased monotonically with the increase of the carbonation temperature. At the carbonation temperatures of 300 and 400 °C, the amount of CO₂ released at the outlet of the methanation reactor was significantly lower than that at 200 °C. Under such conditions (300–400 °C carbonation), the CO₂ yield to methane, based on the CO₂ transferred from the CO₂-capture step, was almost equal to unity. Notably, the CO outlet concentration was negligible under most test conditions explored. Table 1 summarizes the average CO₂ conversion and selectivity to methane (as defined in Section 2.4) for all the conditions tested.

Turning to the Na-promoted DFM, Fig. 8 shows the normalized measured molar flows of outlet CH₄ as a function of time for a test under the same conditions as those shown in Fig. 5 for the Li-promoted DFM

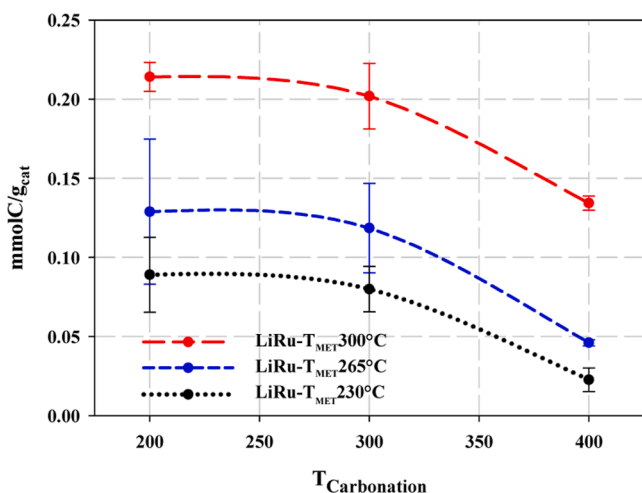


Fig. 7. Overall amount of carbon-containing species at the methanation outlet produced under the ICCR tests conditions with Li-Ru/Al₂O₃ DFM.

Table 1

CO₂ conversion and selectivity to methane during the ICCR tests with Li-Ru/Al₂O₃ DFM as a function of carbonation and methanation temperatures. Data are reported as: X_{CO₂} / S_{CH₄}.

LiRu			
T _{CAR} →	200 °C	300 °C	400 °C
T _{MET} ↓			
230 °C	64 % / 99.9 %	99 % / 94 %	100 % / 86 %
265 °C	76 % / 98.9 %	97 % / 99.9 %	100 % / 100 %
300 °C	62 % / 98.7 %	93 % / 99.6 %	100 % / 100 %
NaRu			
T _{CAR} →	200 °C	300 °C	400 °C
T _{MET} ↓			
300 °C	67 % / 85 %	83 % / 88 %	97 % / 94 %

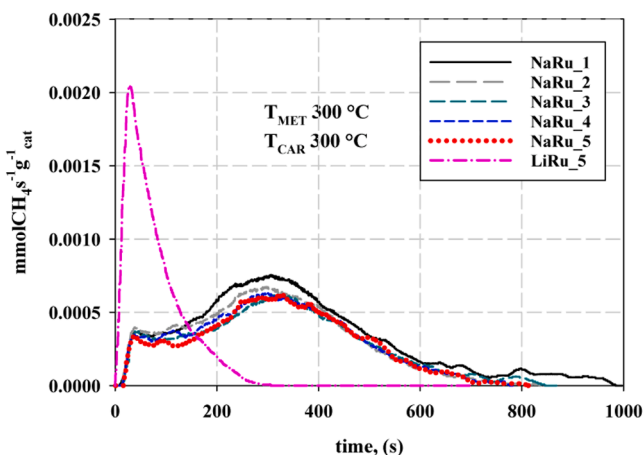


Fig. 8. Temporal normalized CH₄ outlet molar flow for the Na-Ru/Al₂O₃ test at methanation and carbonation temperatures of 300 °C. The curves refer to the 5 methanation cycles, plus the 5th cycle for the Li-Ru DFM.

(one curve taken from Fig. 5 is also reported in the figure, for comparison).

The trend of the curves in Fig. 8 differs from the one presented for the Li-Ru DFM, but still shows good reproducibility over the cycles. In particular, the CH₄ peak production value is significantly lower with respect to the Li-based DFM and delayed to ca 300 s. Due to the slower kinetics of the catalytic reaction, longer times were required to convert all of the pre-captured CO₂ into methane. The overall CH₄ and CO outlet amounts at the methanation temperature of 300 °C and at the different carbonation conditions, are compared in Fig. 9 for the two DFMs considered. For CH₄ the same non-monotonic trend, already explained for the Li-Ru DFM case, occurred, essentially due to the CO₂ stripping caused by the experimental procedure. When the Na-Ru DFM was used, the total amount of produced CH₄ was higher under all the carbonation conditions.

However, the higher methane production observed in the case of the Na-promoted DFM was associated with a higher release of CO (as clearly seen in Fig. 9 and confirmed by the selectivity results reported in Table 1). As regards the overall release of carbon-containing species, reported in Fig. 10, the extent of this release was indeed greater than in the case of the Li-Ru DFM, resulting in lower yield values of 57, 73 and 91 % at a carbonation temperature of 200, 300 and 400 °C, respectively. Compared to the Li-Ru DFM material, apart from the higher CO release, a larger part of the CO₂ captured and transferred from the carbonation reactor was released during the methanation step without reacting with hydrogen, even at the higher carbonation temperatures of 300 and 400 °C, as can be appreciated from conversion data reported in Table 1.

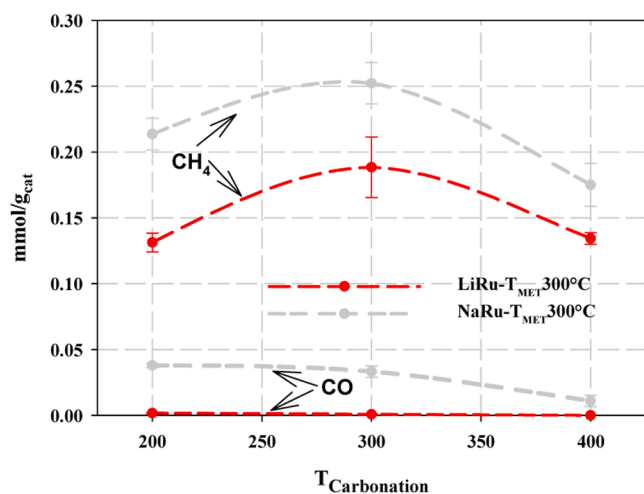


Fig. 9. Overall CH₄ and CO produced at the methanation temperature of 300 °C for the tests with Li-Ru and Na-Ru DFMs at the different carbonation temperatures.

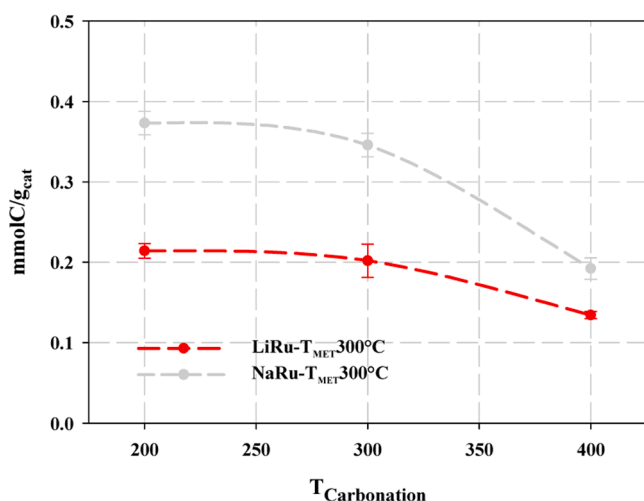


Fig. 10. Overall amount of carbon-containing species at the methanation outlet at 300 °C for the tests with Li-Ru and Na-Ru DFMs at the different carbonation temperatures.

3. Conclusions

In this work, a chemical looping integrated CO₂ capture and reduction (ICCR) process, based on the use of two interconnected fluidized beds, to capture and convert CO₂ from flue gas into CH₄, was investigated. The experimental batch lab-scale apparatus, the Twin Beds system, consisted of two bubbling fluidized beds connected to each other by a duct enabling the fast transfer of solid materials during the CO₂ capture/methanation cycles. The selected dual function materials combining both sorbent and catalytic properties, were prepared by dispersing low loadings of Ruthenium (1 %) and Lithium or Sodium (5 %) over fluidizable γ -Al₂O₃ spheres with high surface area and mechanical resistance. In particular, after each CO₂ capture step, the DFM particles were rapidly transferred in the second reactor where the hydrogenation was carried out in 4 % H₂/N₂ mix to produce CH₄. The process was repeated for a total of 5 complete cycles.

As for the highly performing Li-Ru DFM, the CO₂ capture and methanation phases were carried out in the temperature ranges 200–400 °C and 230–300 °C, respectively. When considering carbonation, as expected for a chemisorption process, the CO₂ uptake decreased with

increasing temperature. For the lowest carbonation temperature of 200 °C, the CO₂ amount released in the nitrogen purge phase before methanation was larger due to desorption occurring when passing to the higher methanation temperature. Thus, higher CO₂ conversions to CH₄ occurred at higher carbonation temperatures. On the other hand, the kinetic constraints of the methanation reaction determined the best performance, in terms of methane yield, at the highest methanation temperature (300 °C). As an overall effect, the optimal condition identified for this set of tests corresponded to the case in which carbonation and methanation occurred at the same temperature of 300 °C. Moving from these findings, the Na-promoted DFM was tested at the methanation temperature of 300 °C. This material presented slower but larger methane production, as well as lower selectivity values and a higher release of unreacted CO₂ in the methanation phase.

Regarding the CO₂ stripping experienced during the tests, it may be worth noting that in a more realistic continuous chemical looping system, the limitation due to such experimental transient phases would not be encountered, and therefore the possibility of decoupling the two processes entails a large potential intensification. In particular, physically separating the adsorption and hydrogenation phases would allow to split the exothermicity of the whole process and to optimize each single step in terms of temperature and other operating parameters.

Finally, regarding the long term durability of the DFMs, in this first work we restricted the testing to only 5 consecutive cycles for each set of conditions aiming to demonstrate the process feasibility and the DFM consistent performance during alternate operation in the interconnected FB reactors. Specifically, we compared two DFM formulations which were already tested in the fixed bed configuration [8,12,16]. It was shown there that both DFMs display a good long-term performance stability during cyclic operation up to 320 °C with realistic simulated flue gases containing O₂, H₂O, and even SO₂. However, no data are yet available regarding DFMs durability under FB conditions: therefore, we plan to explore this topic as the next step of our work.

Novelty and significance statement

The integrated CO₂ capture and methanation process was investigated in a chemical looping configuration using two dual function materials (DFMs) recirculated alternately between two interconnected fluidized bed reactors. Two DFMs (Li-Ru/Al₂O₃ and Na-Ru/Al₂O₃) were used to investigate the effect of CO₂ capture and methanation temperatures, over 5 repeated cycles for each operating condition. The DFMs performance was quite reproducible over the cycles, and the methane yield approached 100 % under the best operating conditions. This study provides the proof-of-concept of the chemical looping configuration which enables a large potential intensification of the process with respect to the state-of-the-art fixed bed operation.

Author contributions

F.M.: performed research, analyzed data, wrote paper draft
 E.M.C.: performed research
 S.C.: designed research, reviewed and edited paper
 A.C.: analyzed data, reviewed and edited paper
 F.S.: designed research, reviewed and edited paper

Declaration of competing interest

The authors declare that they have no known competing financial interests or personal relationships that could have appeared to influence the work reported in this paper.

Acknowledgements

The authors acknowledge funding from the project PNRR - Partenariati estesi - “NEST - Network 4 Energy Sustainable Transition” -

PE0000021.

Fiorella Massa and Elisabetta Maria Cepollaro acknowledge funding from the European Union - NextGenerationEU under the National Recovery and Resilience Plan (NRRP), Mission 04 Component 2 Investment 3.1, Project Code: IR0000027 - CUP:B33C22000710006 - iEN-TRANCE@ENL: Infrastructure for Energy TRAnSition aNd Circular Economy @ EuroNanoLab

References

- [1] M. Gotz, J. Lefebvre, F. Mors, A. McDaniel Koch, F. Graf, S. Bajohr, R. Reimert, T. Kolb, Renewable power-to-Gas: a technological and economic review, *Renew. Energy* 85 (2016) 1371–1390.
- [2] M.S. Duyar, M.A.A. Trevino, R.J. Farrauto, Dual function materials for CO₂ capture and conversion using renewable H₂, *Appl. Catal. B Environ.* 168–169 (2015) 370–376.
- [3] L.F. Bobadilla, J.M. Riesco-García, G. Penélas-Pérez, A. Urakawa, Enabling continuous capture and catalytic conversion of flue gas CO₂ to syngas in one process, *J. CO₂ Utiliz.* 14 (2016) 106–111.
- [4] S. Omodolor, H.O. Otor, J.A. Andonegui, B.J. Allen, A.C. Alba-Rubio, Dualfunction materials for CO₂ capture and conversion: a review, *Ind. Eng. Chem. Res.* 59 (40) (2020).
- [5] S. Bin Jo, J.H. Woo, J.H. Lee, T.Y. Kim, H.I. Kang, S.C. Lee, J.C. Kim, CO₂ green technologies in CO₂ capture and direct utilization processes: methanation, reverse water-gas shift, and dry reforming of methane, *Sustain. Energy Fuel.* 4 (2020) 5543–5549.
- [6] F. Kosaka, Y. Liu, S.-Y. Chen, T. Mochizuki, H. Takagi, A. Urakawa, K. Kuramoto, Enhanced activity of integrated CO₂ capture and reduction to CH₄ under pressurized conditions toward atmospheric CO₂ utilization, *ACS Sustain. Chem. Eng.* 9 (2021) 3452–3463.
- [7] F. Kosaka, T. Sasayama, Y. Liu, S.Y. Chen, T. Mochizuki, K. Matsuoka, A. Urakawa, K. Kuramoto, Direct and continuous conversion of flue gas CO₂ into green fuels using dual function materials in a circulating fluidized bed system, *Chem. Eng. J.* 450 (2022).
- [8] S. Cimino, R. Russo, L. Lisi, Insights into the cyclic CO₂ capture and catalytic methanation over highly performing Li-Ru/Al₂O₃ dual function materials, *Chem. Eng. J.* 428 (2022) 131275.
- [9] M.S. Duyar, S. Wang, M.A. Arellano-Trevino, R.J. Farrauto, CO₂ utilization with a novel dual function material (DFM) for capture and catalytic conversion to synthetic natural gas: an update, *J. CO₂ Utiliz.* 15 (2016) 65–71.
- [10] A. Bermejo-Lopez, B. Pereda-Ayo, J.A. Gonzalez-Marcos, J.R. Gonz'alez-Velasco, Mechanism of the CO₂ storage and in situ hydrogenation to CH₄. Temperature and adsorbent loading effects over Ru-CaO/Al₂O₃ and Ru-Na₂CO₃/Al₂O₃ catalysts, *Appl. Catal. B Environ.* (2019) 117845.
- [11] D.I. Li, N. Ichikuni, S. Shimazu, T. Uematsu, Catalytic properties of sprayed Ru/Al₂O₃ and promoter effects of alkali metals in CO₂ hydrogenation, *Appl. Catal. A Gen.* 172 (2) (1998) 351–358.
- [12] S. Cimino, F. Boccia, L. Lisi, Effect of alkali promoters (Li, Na, K) on the performance of Ru/Al₂O₃ catalysts for CO₂ capture and hydrogenation to methane, *J. CO₂ Utiliz.* 37 (2020) 195–203.
- [13] A. Coppola, F. Scala, L. Gargiulo, P. Salatino, A twin-bed test reactor for characterization of calcium looping sorbents, *Powder Technol.* 316 (2017) 585–591.
- [14] A. Coppola, F. Massa, P. Salatino, F. Scala, Fluidized bed CaO hydration-dehydration cycles for application to sorption-enhanced methanation, *Combust. Sci. Technol.* 191 (2019) 1724–1733.
- [15] C. Jeong-Potter, A. Porta, R. Matarrese, C.G. Visconti, L. Lietti, R. Farrauto, Aging study of low Ru loading dual function materials (DFM) for combined power plant effluent CO₂ capture and methanation, *Appl. Catal. B: Environ.* 310 (2021) 121294.
- [16] S. Cimino, E.M. Cepollaro, L. Lisi, Ageing study of Li-Ru/Al₂O₃ dual function material during the integrated CO₂ capture and methanation with SO₂-containing flue gas, *Carbon Capt. Sci. Technol.* 6 (2022) 100096.